HOKKAIDO UNIVERSITY

Title	Global warming response of snowpack at mountain range in northern Japan estimated using multiple dynamically downscaled data
Author(s)	Katsuyama, Yuta; Inatsu, Masaru; Nakamura, Kazuki et al.
Citation	Cold Regions Science and Technology, 136, 62-71 https://doi.org/10.1016/j.coldregions.2017.01.006
Issue Date	2017-04
Doc URL	https://hdl.handle.net/2115/72482
Rights	©2017 This manuscript version is made available under the CC-BY-NC-ND 4.0 license http://creativecommons.org/licenses/by-nc-nd/4.0/
Rights(URL)	https://creativecommons.org/licenses/by-nc-nd/4.0/
Type	journal article
File Information	manuscript CRST136 62-71.pdf

Hokkaido University Collection of Scholarly and Academic Papers : HUSCAP

Global warming response of snowpack at mountain range in northern Japan estimated using multiple dynamically downscaled data

Yuta Katsuyama[1], Masaru Inatsu[2], Kazuki Nakamura[3], and Sumito Matoba[4]

[1]Graduate School of Science, Hokkaido University; Rigaku 8th bldg., N10W8, Sapporo, 0600810, Japan
[2]Faculty of Science, Hokkaido University; Rigaku 8th bldg., N10W8, Sapporo, 0600810, Japan
[3]National Research Institute for Earth Science and Disaster Resilience; 3-1, Tennodai, Tsukuba, Ibaraki, 3050006, Japan
[4]Pan-Okhotsk Research Center, Institute of Low Temperature Science, Hokkaido University; N19W8, Sapporo, 0600819, Japan

Corresponding author: Mr. Yuta Katsuyama
Phone: +81−11−706−4609
E-mail: katsuyama@sci.hokudai.ac.jp

16 Abstract

17 We estimate the response of snowpack to global warming along with the uncertainty of
18 the snowpack change by using a combination of multiple general-circulation models
19 (GCMs), a single regional atmospheric model, and a one-dimensional multi-layered
20 snowpack model. The target site is Mt. Annupuri in Kutchan, Hokkaido, Japan. The
21 forcing of the snowpack model is taken from dynamically downscaled data from GCMs
22 for the present climate and GCMs in a decade when the global-mean temperature has
23 increased by 2 K from present conditions. The results show that global warming would
24 decrease the monthly-mean snow depth throughout the winter season. Other salient
25 features are the decrease of snow depth by 60 cm with maximum uncertainty of 20 cm at
26 the beginning of the snow ablation period, the occurrence of the snow-depth peak a month
27 earlier, and the dominance of melt forms in an earlier season. The ratio of melt forms for
28 all snowpack layers increase with little uncertainty before the snow ablation period. The
29 ratio of hoar does not change much, even though the air temperature increases. The
30 uncertainty in snowpack evaluation is also discussed.

31

32 Keywords

33 Snowpack modeling; Snowpack change; Snow type change; Uncertainty

1 Introduction

In the present climate, snowpack occurs seasonally in the extratropics and even permanently in mountainous regions, and it is thought to be strongly affected by global warming especially at mid-latitudes. According to the latest report of the Inter-governmental Panel for Climate Change (IPCC), the emission of greenhouse gases leads not only to an increase in air temperature but also changes in wind, precipitation amount and intensity, and cloudiness (Stocker et al., 2014). The temperature is one of the most important variables controlling the amount of snow, the properties of snowpack, and the snow cover period, because snow and ice are retained below freezing but rapidly melt above this temperature (López-Moreno et al., 2008, 2013). Moreover, wintertime snowfall, which represents the major contribution to total snow accumulation, is frequently observed in storm-track areas, such as northern Europe, northeastern America, and northern Japan. Because this snowfall is often caused by extratropical cyclone passage, it might be changed by global warming. The physical properties of snowpack might be also changed as a result of efficient transformation from solid precipitation particles to melt forms in a warmer climate. This transformation of grain types may also change the occurrence of wet-avalanche because that of wet-avalanche is related to the wetting of snowpack (Mitterer et al., 2011). Although the

53 wet-avalanche sometimes occurs in Japan (Akitaya et al., 2015) and changes of the
54 wet-avalanche occurrence have been pointed out in the North America (Lazar and
55 Williams, 2008) and in France (Castebrunet et al., 2014), the transformation of grain
56 types responding to the global warming in Japan is not well addressed. Moreover,
57 considering the utilization of water resources (Beniston, 2003), the mitigation of snow
58 disaster (Nakai et al., 2012), and winter tourism (Beniston, 2003; Uhlmann et al., 2009),
59 the impact of climate change on snowpack dynamics deserve to be examined (e.g.
60 Niwano et al., 2012; Mellander et al., 2007; Inatsu et al., 2016), even though there is
61 still inherent uncertainty in models of the impact of climate change.

62 We found several studies of snowpack response to climatic change, such as an
63 estimation of snowpack including its physical property along with its uncertainty by the
64 use of one-dimensional and multi-layered snowpack model (e.g. Rasmus et al., 2004;
65 Lazar et al., 2006; Rousselot et al., 2012). They consist mostly of three steps: (i) climate
66 change projection with atmosphere–ocean general-circulation models (GCMs), in which
67 atmospheric concentrations of greenhouse gases are prescribed as a function of year
68 (Solomon et al., 2007; Stocker et al., 2014); (ii) downscaling, which creates climatic
69 variables at a particular site or in a limited area with higher spatial resolution in order to
70 compensate for the insufficient resolution of GCMs (Wang et al., 2004; Wilby et al.,

71 2004); and (iii) snowpack estimates, either with a physical model (e.g. Rasmus et al.,
72 2004) or with a statistical relation that has been empirically determined in advance
73 (Inoue and Yokoyama, 1998). For step (i), there are no other technical choices than
74 using GCMs. The GCM projection introduces an uncertainty in evaluating global-mean
75 temperature, however, because of differing climate sensitivities among GCMs, mainly
76 due to their physical parameterizations, and because future greenhouse gas emissions
77 depend on the socio-economic scenario (Stocker et al., 2014). The GCM projections of
78 wintertime temperature and precipitation at a particular mid-latitude site are also
79 uncertain, due to uncertain changes in storm tracks and jet streams at mid-latitudes
80 (Chang et al., 2012), wintertime Asian monsoon (Ogata et al., 2014), and the Arctic
81 Oscillation (Karpechko, 2010). These regional climate patterns certainly affect snow
82 accumulation and melt dynamics, and also snowpack dynamics. It should be noted that
83 GCMs are more or less biased, so one needs a bias correction for a particular site. One
84 then proceeds to step (ii) based on coarse-resolution GCM projection with uncertainty
85 and bias. The methods of step (ii) can be classified into dynamical downscaling (DDS)
86 (Wang et al., 2004) and statistical downscaling (Wilby et al., 2004). The former
87 provides higher-resolution climatic variables in a limited area by integrating a regional
88 atmospheric model (RAM) with the GCM output imposed as its lateral boundary

89 condition. The latter estimates a future state by simply applying a statistical relation
90 between local-site information and weather patterns such as the Siberian-Japan pattern
91 that brings much snowfall along the Japan Sea side of northern Japan (Takano et al.,
92 2008). The Siberian-Japan pattern is established based on the singular-value
93 decomposition analysis between synoptic weather pattern and local precipitation, for
94 example (Kuno and Inatsu, 2014). Recently, DDS has been widely used in the
95 community, in spite of the need for additional computation, because it has the ability to
96 produce a physically consistent dataset (e.g. Wang et al., 2004; Kuno and Inatsu, 2014;
97 Inatsu et al., 2015). Multiple RAMs, even with a single GCM imposed as the lateral
98 boundary condition, also provide uncertainty, mainly due to the variability among the
99 RAMs' physical parameterizations, but the uncertainty is not large for the extratropics in
100 winter because the DDS results are strongly controlled by lateral boundary conditions
101 (Inatsu et al., 2015; Kuno and Inatsu, 2014). In step (ii) when using DDS, a bias
102 correction should be made just before step (iii) because the DDS results have the
103 systematic biases in atmospheric variables such as temperature, precipitation, and so on,
104 due to physical parameterizations and resolution (Ishizaki et al., 2012). It should be
105 noted that an alternative choice in step (ii) is the pseudo-global warming (PGW)
106 experiment, in which observed weather time-series are added to the climatological

107 difference estimated from GCM integrations so as to form the lateral boundary
108 condition of the RAM (Kimura and Kitoh, 2007). Finally step (iii) estimates the future
109 snowpack change, which is still a challenging problem. Although Inoue and Yokoyama
110 (1998) estimated maximum snow depth and major snow type over Japan by using a
111 statistical relation between snowpack and meteorological characteristics, recent studies
112 have tended to use one-dimensional multi-layered snowpack models, such as CROCUS
113 (Brun et al., 1992), SNTHERM (Jordan, 1991), and SNOWPACK (Bartelt and Lehning,
114 2002) and its modification for wet-heavy snow (Hirashima, 2014). A one-dimensional
115 multi-layered snowpack model enables us to calculate the temporal evolution of
116 snowpack structure with multiple layers at a particular site, driven by atmospheric
117 variables, such as air temperature, precipitation, humidity, wind, and shortwave
118 radiation at the snow surface. Step (iii) is, therefore, undertaken on the basis of
119 bias-corrected atmospheric variables obtained from step (ii).

120 Several previous studies have been devoted to an evaluation of future
121 snowpack change for particular areas, such as Switzerland (Bavay et al., 2009, 2013),
122 Finland (Rasmus et al., 2004), France (Rousselot et al., 2012), and North America
123 (Lazar et al., 2006). Basically, uncertainty in future snowpack was estimated under
124 multiple emission scenarios of greenhouse gases. The emission scenario strongly

125 controls the global-mean temperature increase, a factor to which snowpack estimation is
126 sensitive. For example, Rousselot et al. (2012) revealed that the snow water equivalent
127 change in the A2 scenario of the Special Report on Emissions Scenarios (SRES) was
128 double to that in the B1 scenario. Bavay et al. (2009) also pointed out a great
129 discrepancy between results for the A2 and B2 scenarios. Moreover, under the same
130 emission scenario, different GCMs provide different global-mean temperature increases
131 due to climate sensitivity. The use of multiple GCMs, therefore, increases the range of
132 estimates of future snowpack (Bavay et al., 2013; Lazar et al., 2006; Rasmus et al.,
133 2004).

134 When considering the effect of climate change on snowpack, one may desire
135 to separate the changes due to differences in global-mean temperature from those due to
136 changes of synoptic-scale climate around a particular site. However, since the
137 temperature increase affects snowpack estimation quite strongly, it is difficult to
138 determine the uncertainty arising from changes of meso-scale convection, storm tracks,
139 and quasi-stationary pressure patterns by using a set of arbitrarily chosen GCMs.

140 From the point of view of numerical snowpack experiments, biased input data
141 can cause problems. For example, a warm bias would shorten the snow season and a dry
142 bias would effectively decrease the snow depth. Hence, we need a rational treatment for

bias in GCMs and downscaled data. One way to ameliorate this problem is to offset climatological differences between present and future conditions assuming that the model biases are stationary. This approach has been used in several studies. Rasmus et al. (2004) calculated the snowpack difference for present and future climates using DDS without any bias correction of input data. Bavay et al. (2009; 2013) and Nakamura et al. (2011) estimated a change in snowpack using the PGW strategy. It is also expected that statistical downscaling will correct for any bias without requiring additional procedures (Rousselot et al., 2012; Lazar et al., 2006).

The purpose of this study is to estimate future snowpack evolution along with its uncertainty by a combination of multiple GCMs, a single RAM, and a one-dimensional snowpack model (Fig. 1). The analysis is based on the idea proposed in Inatsu et al. (2015), in which the synoptic-scale response was successfully separated from global temperature increase by performing DDS for a decade during which the global-mean surface air temperatures increase by 2 K. Here, we use the dataset archived by Kuno and Inatsu (2014) and skip steps (i) and (ii) of the procedure in Fig. 1. In pre-processing before the snowpack calculation, we make bias corrections for temperature and precipitation and height correction for temperature in order to discuss differences of the snowpack response with altitude. After pre-processing, the numerical

161 snowpack calculation is performed for a particular mountain range at Mt. Annupuri in
162 Kutchan, Hokkaido, Japan (Fig. 2).

163 This paper is organized as follows. Section 2 describes the study area
164 including its climate. Section 3 briefly describes the observation, the downscaled data,
165 and the model for numerical snowpack calculation together with the bias correction
166 method. Section 4 shows the snowpack results for downscaled data under present and
167 future climates. We also present the uncertainty of the estimates by using multiple
168 GCMs. Section 5 discusses how the results can be interpreted. Finally, section 6 gives
169 the conclusion.

170

171 2 Study area

172 We chose Mt. Annupuri as a particular mountain range for three reasons. First,
173 the climate at the site is categorized as Dfb in the Köppen-Geiger climate classification
174 characterized by cold, no dry season, and warm summer (Peel et al., 2007). The
175 climatological air temperature is −4.7 °C and total precipitation attains 500 mm in
176 December–February at the observation site of the Japan Meteorological Agency (JMA)
177 in Kutchan. The snowfall is heavier than other areas around Kutchan because
178 moisture-rich air produced above the sea is advected by winter monsoonal wind (e.g.

Takano et al., 2008). The climatological feature holds the snow-cover period exceeding 4 months and a maximum snow depth of 190 cm even at the mountain base. Second, this site encompasses the mountain top, at 1,308 m above sea level, down to a wide steep hill with its base around 200 m above sea level (Fig. 2b). The large difference of height at a single mountain enables us to facilitate the discussion on snowpack change with different temperature baselines. For the estimation, we considered three locations: the top (1,300 m), the hillside (800 m), and the base (173 m), which is the level of the JMA's meteorological station (Fig. 2b). The site is the downwind side of winter monsoon that brings heavy snowfall. The slope of Mt. Annupuri directs from southwest to northeast and the part of mountain area is leeward, but we do not consider the effect of such small-scale topography on the mountain slope. Finally, there is a social demand for the estimation because a famous ski resort with high-quality snow is located at the site.

3 Data and Methods

3.1 Data

3.1.1 Downscaled data

We used a dataset of DDS results provided by Kuno and Inatsu (2014). For

197 this dataset, the 1990s in the 20th century experiment (20C3M) was chosen as a period
198 of present climate. Periods of future climate were the decades in which each GCM
199 estimated the global-mean surface air temperature increase by 2 K under the SRES A1b
200 condition compared with the present climate. This selection of the different decades
201 may distinguish the uncertainty due to changes in synoptic phenomena from the
202 uncertainty due to the climate sensitivity and emission scenario (Inatsu et al., 2015).

203 In the DDS, three GCMs of the Coupled Model Inter-comparison Project
204 phase 3 (CMIP3) were chosen as initial and boundary conditions for a RAM of the
205 JMA/Meteorological Research Institute (JMA/MRI) nonhydrostatic model (Saito et al.,
206 2006). The chosen GCMs were the high-resolution version of the Model for
207 Interdisciplinary Research on Climate 3.2 (MIROC; Hasumi and Emori, 2004), the
208 fifth-generation atmospheric GCM of the Max-Planck-Institut für Meteorologie
209 (ECHAM5/MPI; Roeckner et al., 2003), and version 3 of the Community Climate
210 System Model of the National Center for Atmospheric Research (CCSM3/NCAR;
211 Collins et al., 2006). These three GCMs were able to reproduce the present climate
212 around Hokkaido (Kuno and Inatsu, 2014). As for the RAM, the spatial resolution was
213 10 km and the domain size was ~2.1×10^6 km^2, ranging from 135°E to 150°E and 39°N
214 to 49°N. Mt. Annupuri is not resolved in the topography of the RAM (Fig. 2a). The

DDS was performed for the present climate of 1990s for all three GCMs. The DDS was also performed for the 2050s for MIROC, the 2060s for the MPI model, and the 2080s for the NCAR model, these being the decades in which each GCM estimated that the global-mean surface temperature would have increased by 2 K. For the snowpack calculation, the DDS data corresponding to the nearest grid point to the study area approximately including the three locations of the top, hillside, and base in the same single grid, are used as atmospheric forcing (Fig. 2b). Although the selected grid do not include the base point (Fig. 2b), it is used as the forcing because the same observation data should be used for the bias correction of the following section 3.2. Forced variables are temperature, precipitation, relative humidity, incoming shortwave radiation, and wind.

3.1.2 Observed data

The temperature, precipitation, relative humidity, incoming shortwave radiation, wind, and snow depth observed with the Automated Meteorological Data Acquisition System (AMeDAS) operated by the JMA are basically used for validation of snowpack modeling. The validation was done at Sapporo, because all the meteorological data necessary for the snowpack model run have been operationally

observed there, and because a snow pit observation twice a week at Sapporo (Niwano et al., 2012) enables us to validate the model. This snow pit observation measured the grain type of snowpack in depth; the type is classified into precipitation particles, graupel, decomposed precipitation particles, rounded grains, faceted crystals, depth hoar, ice formations, crust, and melt forms. Note that faceted crystals and depth hoar are regarded as a single type of hoar in this study. The temperature and precipitation of AMeDAS data at Kutchan were used for the bias correction for downscaled data.

3.2 Pre-processing of the forcing data

Bias corrections for DDS precipitation and temperature of data are made by comparing present-climate simulations with the JMA's observations at the base point. A temperature bias is defined monthly as the DDS-data climatology minus the observed climatology, and the bias is simply subtracted from the hourly DDS data. The temperatures at the hillside point and at the mountain top point are estimated by the temperature difference from the base decreased by means of the standard lapse rate of 6.5 K/km. As for precipitation, the scaling factor to correct the DDS data is determined month by month from the observed climate at the base point. This scaling factor is loaded for all the downscaled data (Prudhomme et al., 2002). We assumed no difference

of precipitation among top, hillside, and base points, because no reference data are available for the hillside and top points. We did not make any pre-processing for other climatic variables.

3.3 SNOWPACK model setup

We used version 3.2.1 of SNOWPACK for step (iii) in the procedure (Fig. 1). SNOWPACK is based on a one-dimensional multi-layered snowpack model and solves the mass balance for water vapor, liquid water, and snow, and the energy balance for snowpack. See Bartelt and Lehning (2002) for more details. This model has some achievement to be applied to Japan and have been suitable for cold regions including Hokkaido (Hirashima et al., 2004; Nakamura et al., 2011; Nishimura et al., 2005). This study applied the NIED scheme (Hirashima et al., 2010) for a better representation of the wet, heavy snow typically observed in Japan. We forced this model with hourly meteorological data of air temperature, relative humidity, wind speed, incoming shortwave radiation, and precipitation at the snow surface. Snowfall is discriminated from rainfall according to a threshold of 1.2 ℃ in surface air temperature and a threshold of 50% in relative humidity in the model. The volume of precipitation particles is estimated from precipitation with a snow density parameterization slightly

269 modified from that in Lehning et al. (2002a), but this modification is unpublished. Net
270 longwave radiation is estimated from externally given air temperature and snow surface
271 temperature as calculated in the model, because incoming longwave radiation is not
272 prescribed (Lehning et al., 2002a). The soil temperature is fixed at 0 °C. Latent and
273 sensible heat fluxes from snow surface to air are calculated under the Monin–Obukhov
274 bulk formulation (Monin and Obukhov, 1954). The integration period for a single
275 season is from 1 October of a year to 25 June in the following year, and the 10-season
276 integration is done for bias-corrected downscaled data with a particular GCM under
277 present or future climate.

278 In SNOWPACK, snow grains are classified into eight types with majority and
279 minority forms: precipitation particles, decomposed precipitation particles, rounded
280 grains, faceted crystals, depth hoar, surface hoar, ice formations, and melt forms
281 (Lehning et al., 2002b). The snow grain type is determined by four parameters in the
282 model: dendricity, sphericity, grain size, and grain type history. Precipitation particles
283 have higher dendricity; rounded grains are characterized by higher sphericity, while
284 faceted crystals are characterized by low sphericity. This study regards faceted crystals,
285 depth hoar, surface hoar, and their mixed forms, which were originally differentiated in
286 the model, as a single type of hoar. We also ignore the minority forms. This study

focuses on only the ratios of melt forms and hoar as traditional indices of snowpack property, which can be readily validated by a comparison with the snow pit observation because number of layers observed is different with that of layers calculated. The ratio of melt form is useful to diagnose wet avalanches (Techel and Pielmeier, 2010), while the hoar is recognized as one of the factors for dry avalanches at Mt. Annupuri (Nishimura et al., 2005). In the following sections, we define the date of maximum snow depth as the boundary between the “accumulation period” and the “ablation period”.

3.4 Sensitivity experiment

This paper has basically excluded the effect of small-scale topography on the mountain slope and assumed the uniform precipitation field among top, hillside and base points in the pre-processing (section 3.2), mainly because we have no reference data of precipitation at top and hillside points. However, even the small-scale topography more or less contributes to the total amount of precipitation (Houze, 2012), so that the amount depends on the points where we address. Therefore we conduct an additional sensitivity experiment to precipitation at the top in order to discuss an influence of the possible orographic effects on the snowpack estimation. In this

sensitivity experiment, the snowpack model ran with the same downscaled data except for hourly precipitation data increasing or decreasing by 20%.

4 Results

4.1 Atmospheric changes

Figure 3 shows the global warming response of the monthly-mean temperature and monthly precipitation at Kutchan. Although the future climate is defined as the decades when global-mean temperature has increased by 2 K compared with 1990s, the DDS results showed a temperature increase of about 2.5 K, probably because of land-sea contrast in the Northern Hemisphere. Remember that DDS with MIROC, MPI, and NCAR GCMs was performed for the future periods of 2050s, 2060s, and 2080s, respectively, and they are compared with the reference of present climate. The DDS results from MIROC show the least month-to-month variation while the NCAR GCM shows the most; the amount of increase is slightly smaller in the MPI case. The precipitation change also has a large seasonal variation, but the total amount of wintertime precipitation does not increase. There is a small tendency toward increased precipitation in January and April, however.

323 4.2 Validation of the model

324 We validated the SNOWPACK model by comparing the calculations enforced
325 by the atmospheric variables observed at Sapporo with the snow data observed at
326 Sapporo. Figure 4 shows some snowpack properties at Sapporo for three winters of
327 2009/2010, 2010/2011, and 2011/2012 (The winter season is between December and the
328 following May). Snow depth is well simulated through the season, except for a slight
329 overestimation in March and April 2011 (Figs. 4a‑c). The ratio of melt forms for all
330 snowpack layers is also well simulated, but the simulated ratio in December and January
331 2011/12 is twice larger than the observed ratio (Figs. 4d‑f). The ratio of hoar is
332 overestimated as well, especially in 2010/11 (Figs. 4g‑i). SNOWPACK cannot
333 reproduce the hoar realistically as in our experiments, presumably because snowpack
334 surface temperature tends to decrease in the model. It is remarked, however, that we will
335 show the results of hoar by regarding it as the diagnosed quantity that is a function of
336 temperature gradient inside of the snowpack (Lehning et al., 2002b).

337 The simulated snow depth at the base point with present-climate downscaled
338 data at the nearest grid point to Mt. Annupuri is also compared with the snow depth
339 observed at the JMA observatory at Kutchan. Recall that DDS temperature and
340 precipitation data are bias-corrected but other climatic variables are not. The

341 monthly-mean snow depth is highly correlated with the observations, though it is
342 slightly underestimated in February to March and overestimated in April (Fig. 5a). This
343 overestimation is consistent with an earlier report on the snow ablation period in the
344 Japanese snowy area (Yamaguchi et al., 2004). It is also remarked that, though the
345 validation of the snow depth at the hillside and top points was basically difficult for the
346 paucity of observation, the special observation at the hillside by Nishimura et al. (2005)
347 did not give much difference from our simulated result described below.
348
349 4.3 Snowpack estimation
350 Figure 5 shows the snowpack estimations based on DDS under the present
351 climate. The monthly-mean snow depth attains seasonal maximums of 130 cm at the
352 base point, 190 cm at the hillside point, and 220 cm at the top point. The maximum
353 monthly-mean snow depth increases by about 8 cm per 100 m in altitude. In addition,
354 the greatest depth occurs later at higher altitudes because the freezing environment
355 extends the snowfall period.
356 Global warming significantly decreases monthly-mean snow depth at all
357 points throughout the season (Fig. 6). From December to February, the snow depth
358 decreases by 30 cm at the base and hillside points and by 20 cm at the top point,

359 because the beginning of snow season is retarded by a warmer climate. The decrease is
360 then larger for the snow ablation period. The snow depth decrease likely exceeds 60 cm
361 at the base in March, at the hillside in April, and at the top in May because the snow
362 ablation period starts much earlier: the time of greatest snow depth is shifted by about a
363 month. These are consistent with obtained a set of PGW experiments for another site
364 near Sapporo (Nakamura et al., 2011).

365 Figure 7 shows the monthly-mean ratio of melt forms for all snowpack layers
366 in the simulation. Under the present climate, at the base point, melt forms occupy about
367 20% of all snowpack in November, and the ratio gradually increases throughout the
368 season. This pattern does not change substantially under the future climate, but the
369 increase is slightly faster and the melt forms become dominant about a month earlier.
370 Under the present climate, the hillside and top points have a ratio of melt forms that is
371 about 10–20% during the snow accumulation season. Since snow ablation starts earlier
372 in the future, melt forms are dominant at the hillside point in March, and at the top point
373 between March and April. This is also about a month earlier than in the present-climate
374 case.

375 Figure 8 shows the ensemble mean of the monthly-mean ratio of hoar. Under
376 the present climate, at the base point, the ratio of hoar is approximately constant, at

around 10%, from December to March, and the ratio rapidly declines in the snow-melting months. This pattern is also found in the future climate, but the ratio in mid-winter decreases down to 7%. At the hillside point, the ratio of hoar gradually decreases from March to May under the present climate. The percentage is slightly less in the future-climate case. The ratio of hoar is about 15% at the top point from January to April under the present climate. Interestingly, the future-climate case shows no decrease in the ratio of hoar throughout the season at the top point, though the atmospheric warming weakens the temperature gradient in the snowpack. This may be partly because a temperature increase would have little effect on the physical properties of the snowpack in a sufficiently low temperature environment. This is in line with Inoue and Yokoyama (1998), suggesting that global warming would not reduce hoar in eastern Hokkaido.

4.4 Uncertainty

There is fundamentally little uncertainty in the effect on snow depth of global warming because we ruled out the uncertainty associated with climate sensitivity and the emission scenario (Fig. 6). The snow ablation period is uncertain to some extent, however. For example, the difference in snow depth ranged from 30 to 40 cm in January

395 at the base, primarily because precipitation change is insignificant in the MIROC case
396 and +25% in the MPI and NCAR cases (Fig. 3). Although the given climatic variables
397 in February have less variation among GCM cases, the snow accumulation process may
398 increase the variation of the snow-depth difference; it becomes largest at the snow
399 ablation period (Fig. 6a). The uncertainty in the snow-depth difference at the hillside
400 and top points is also noticeable after March (Figs. 6b, c).

401 The ratio of melt forms from base to top points before the snow ablation
402 period has a comparable variation among GCMs for both present and future climates
403 (Figs. 7a, b). However, the variation at the base point in November is relatively larger in
404 the future climate. This is probably because a greater temperature increase (Fig. 3)
405 promoted the deformation to melt forms in a relatively warm temperature environment
406 for the MIROC case. In the snow ablation period, the uncertainty in melt forms tends to
407 increase in the future. The ratio at the top in March ranges between 10% and 20% in the
408 present climate but between 20% and 40% in the future (Fig. 7c). The future-climate
409 uncertainty in March is as much as the present-climate uncertainty in April. This timelag
410 of the uncertainty could be related to the earlier start of melting period.

411

412 4.5 Sensitivity experiment

413 The results of sensitivity experiment are shown in figure 9 and 10. As a matter
414 of course, the monthly-mean snow depth increased (decreased) when precipitation
415 uniformly increased (decreased). In the present climate, for example, the snow depth on
416 March added 30 cm more than the reference in +20% precipitation experiment (Figs. 5c,
417 9a). Because hoar is strongly related to the temperature gradient in snowpack, the ratio
418 of hoar is also sensitive to precipitation (Fig. 10). However, the difference of the snow
419 depth between present and future climate is basically not sensitive to precipitation
420 baseline (Fig. 9b). Similarly, neither the difference of the hoar ratio nor that of melt
421 form is sensitive (Figs. 9c,d,10). The sensitivity experiment then revealed that a
422 systematic tendency of precipitation at a particular point on the mountain slope might
423 only have a secondary effect to the result on the future snowpack change presented here.

424

425 5 Discussion

426

427 This study has estimated the snowpack response to the global-warming
428 atmosphere in the timing where the global-mean temperature would increase by 2 K.
429 According to the IPCC report (Solomon et al., 2007), the climate sensitivity is 4.3 K in

MIROC, 3.4 K in MPI's GCM, and 2.7 K in NCAR's GCM. The uncertainty in greenhouse gas emissions could also cause a large uncertainty in future surface temperature. In our strategy, fixing the temperature increase by the use of a different decade for each model, we have described the snowpack simulation in a "+2-K world." However, the uncertainty in temperature increase could be linked with the simulated points at different altitudes if the standard atmospheric lapse rate were applied. The temperature difference between hillside and top points is 3 K. Moreover the snow-depth difference between the points is about 30 cm (Figs. 5b, c). This means that a 1-K uncertainty in temperature increase approximately corresponds to a 10-cm uncertainty in monthly-mean snow depth at Mt. Annupuri.

Returning to the discussion of climate sensitivity, if we fixed the decade to the 2050s under the A1b scenario, the uncertainty in temperature among GCMs is 1 K (Solomon et al., 2007; Inatsu et al., 2015) so the uncertainty in snow depth would be 10 cm at Mt. Annupuri because a 1-K uncertainty corresponds to a 10-cm uncertainty. Similarly, by fixing the decade to the 2050s again but taking the average over GCM ensembles, the uncertainty in temperature is 0.6 K between A1b and B1 scenarios around Japan (Shin et al., 2012) so the uncertainty in snow depth would be about 6 cm.

The uncertainty in the snow depth is affected by the uncertainty not only in

448 the temperature increase but also in precipitation change among GCMs and among the
449 scenarios. Now, the uncertainty in the snow depth affected by the uncertainty in
450 precipitation is also roughly estimated by the similar way to the above discussion. First,
451 the uncertainty in precipitation change among GCMs around Japan is approximately 0%
452 to +15% if we fixed the decade of the 2050s under the A1b scenario (Shin et al., 2012).
453 Because a +20% uncertainty in precipitation change approximately corresponds to a
454 30-cm uncertainty (Fig. 9a), the uncertainty in snow depth is also about 20 cm. In spite
455 of this relation, the uncertainty in the snow depth would not be affected by the
456 uncertainty in precipitation change among the scenarios because its uncertainty is less
457 than a few percent if we fixed the decade of the 2050s (Shin et al., 2012).

458 Moreover, the source of the uncertainty of snowpack change in the +2 K
459 world may be separated into the uncertainty of temperature increase and others. The
460 temperature increases of the three GCM's cases approximately show a variety of 1 K
461 throughout the season (Fig. 3). Because a 1-K uncertainty in temperature increase
462 approximately corresponds to 10-cm uncertainty in the snow depth, the temperature
463 variation of 1 K may produce a 10-cm uncertainty in the snow depth decrease. Now, the
464 uncertainty in the snow depth decrease at the top point is approximately 25 cm
465 throughout the season (Fig. 6c), so that 40% of the uncertainty is considered to be

466 affected by the uncertainty in the temperature increase. Considering the large sensitivity
467 of snowpack to temperature and precipitation (López-Moreno et al., 2008; 2013),
468 residual uncertainty of 60%, i.e. 15-cm uncertainty, may be mainly produced by the
469 uncertainty in the precipitation. Similarly, at the base and hillside points, 65% and 35%
470 of the uncertainty may be produced by the uncertainty in the temperature and
471 precipitation, respectively.

472 This study could also be applied to avalanches at the site. The wet-avalanche
473 in Switzerland often occurs at the timing of first wetting of snowpack and the arrival of
474 melt-water at the bottom (Mitterer et al., 2011). Because melt forms are produced after
475 some parts of the snowpack become wet (Lehning et al., 2002b), a season when melt
476 forms rapidly increase roughly corresponds to a season of wet-avalanche. For Mt.
477 Annupuri, the snowpack model indicates that a season of wet-avalanche under the
478 global warming is at hillside height after February and at the top after March,
479 respectively, probably because melt forms are produced after some parts of the
480 snowpack become wet. Since the dominance of melt forms arrives earlier according to
481 our evaluation of global warming response (Fig. 7), we speculate that wet avalanches at
482 Mt. Annupuri would be likely to occur in an earlier season. As we introduced in section
483 1, an earlier season of wet-avalanche has been also pointed out in the North America

(Lazar and Williams, 2008) and in France (Castebrunet et al., 2014). It should be noted that it is still uncertain whether this expected shift of wet-avalanche season can be simply applied to Japanese environment.

6 Conclusions

We have evaluated the response to global warming of snow depth and some physical properties of snowpack at the mountain range of Mt. Annupuri in Kutchan, Hokkaido, Japan (Fig. 1), by integrating a numerical snowpack model forced by DDS data with multiple GCMs. First, we validated the numerical snowpack model by comparing the results of the hindcast simulation with observation at Sapporo (17 m above sea level) in three winters of 2009/10, 2010/11, and 2011/12: in particular, we successfully reproduced snow depth at the site with bias-corrected DDS data. The numerical snowpack calculation under present and future climates suggests that monthly-mean snow depth will decrease by about 60 cm at the beginning of ablation period if the global- and local-mean temperature increases by 2 K and approximately 2.5 K, respectively (Figs. 3, 6). In addition, monthly-mean snow depth reaches its peak about one month earlier. The monthly-mean ratio of melt forms tends to increase at all sites, especially above the hillside point, while the monthly-mean ratio of hoar is likely

to decrease except at the top point.

Acknowledgments

The authors thank two anonymous reviewers, Dr. H. Hirashima, Dr. S. Yamaguchi, Prof. S. Minobe, and Dr. Y. N. Sasaki for giving us insightful comments on our earlier results. The snow pit data at Sapporo were collected by the Institute of Low Temperature Science of Hokkaido University and the JMA/MRI. The AMeDAS data are provided by the JMA. This study is supported by Grant-in-Aid for Scientific Research 26310201, and the Social Implementation Program for Climate Change Adaptation Technology, both funded by Ministry of Education, Culture, Sports, Science and Technology. Topography of Fig. 2b is drawn from National Land Numerical Information provided by Ministry of Land, Infrastructure, Transport and Tourism/National Spatial Planning and Regional Policy Bureau of Japan. Some other figures were drawn using the Grid Analysis and Display System.

518 References

519 Akitaya, E., M. Abe, S. Ikeda, K. Izumi, O. Oikawa, H. Ohnishi, T. Ozeki, I. Kamiishi,
520 K. Sakakibara, D. Sasaki, K. Nakamura, K. Nishimura, K. Funaki, and S.
521 Yamaguchi, 2015. Sangaku-Nadare-Taizen, Sangaku-Taizen series 4, edited
522 by Snow Damage Research Team, Japan, pp. 335 (in Japanese).

523 Bartelt, P., and M. Lehning, 2002. A physical SNOWPACK model for the Swiss
524 avalanche warning. Part I. numerical model. Cold Reg. Sci. Technol. 35 (3),
525 123‑145, doi: 10.1016/s0165-232x(02)00074-5.

526 Bavay, M., T. Gruenewald, and M. Lehning, 2013. Response of snow cover and runoff
527 to climate change in high Alpine catchments of Eastern Switzerland. Adv.
528 Water. Resour. 55, 4‑16, doi: 10.1016/j.advwatres.2012.12.009.

529 Bavay, M., M. Lehning, T. Jonas, and H. Lowe, 2009. Simulations of future snow cover
530 and discharge in Alpine headwater catchments. Hydrol. Process. 23 (1), 95‑
531 108, doi: 10.1002/hyp.7195.

532 Beniston, M., 2003. Climatic change in mountain regions: A review of possible impacts.
533 Climatic Change 59, 5‑31, doi: 10.1023/A:1024458411589.

534 Brun, E., P. David, M. Sudul, and G. Brunot, 1992. A numerical-model to simulate
535 snow-cover stratigraphy for operational avalanche forecasting. J. Glaciol. 38

(128), 13‑22, doi: 10.3198/1992JoG38-128-13-22.

Castebrunet, H., N. Echert, G. Giraud, Y. Durand, and S. Morin, 2014. Projected changes of snow conditions and avalanche activity in a warming climate: the French Alps over the 2020-2050 and 2070-2100 periods. The Cryosphere 8, 1673‑1697, doi: 10.5194/tc-8-1673-2014.

Chang, E. K. M., Y. Guo, and X. Xia, 2012. CMIP5 multimodel ensemble projection of storm track change under global warming. J. Geophys. Res. 117, D23118, doi: 10.1029/2012JD018578.

Collins, W. D., C. M. Bitz, M. L. Blackmon, G. B. Bonan, C. S. Bretherton, J. A. Carton, P. Chang, S. C. Doney, J. J. Hack, T. B. Henderson, J. T. Kiehl, W. G. Large, D. McKenna, B. D. Santer, and R. D. Smith, 2006. The Community Climate System Model version 3 (CCSM3). J. Clim. 19 (11), 2122‑2143, doi: 10.1175/jcli3761.1.

Hasumi, H., and S. Emori, 2004. K-1 coupled GCM (MIROC) description Report, CCSR, University of Tokyo, Tokyo, Japan, 34 pp.

Hirashima, H., 2014. Success and challenges of avalanche prediction using numerical snowpack model. Seppyo 76 (6), 411‑419 (in Japanese with English abstract).

Hirashima, H., K. Nishimura, E. Baba, A. Haghikubo, and M. Lehning, 2004.

554 SNOWPACK model simulations for snow in Hokkaido, Japan. Ann. Glaciol.
555 38(7), 123‑129, doi: 10.3189/172756404781815121.
556 Hirashima, H., S. Yamaguchi, A. Sato, and M. Lehning, 2010. Numerical modeling of
557 liquid water movement through layered snow based on new measurements of
558 the water retention curve. Cold Reg. Sci. Technol. 64 (2), 94‑103, doi:
559 10.1016/j.coldregions.2010.09.003.
560 Houze, R. A., Jr., 2012. Orographic effects on precipitating clouds. Rev. Geophys. 50,
561 RG1001, doi: 10.1029/2011RG000365.
562 Inatsu, M., T. Sato, T. J. Yamada, R. Kuno, S. Sugimoto, M. A. Farukh, Y. N. Pokhrel,
563 and S. Kure, 2015. Multi-GCM by multi-RAM experiments for dynamical
564 downscaling on summertime climate change in Hokkaido. Atmos. Sci. Let. 16
565 (3), 297‑304, doi: 10.1002/asl2.557.
566 Inatsu, M., J. Tominaga, Y. Katsuyama, and T. Hirota, 2016. Soil-frost depth change in
567 Eastern Hokkaido under +2 K-world climate scenarios. SOLA 12, 153‑158,
568 doi: 10.2151/sola.2016-032.
569 Inoue, S., and K. Yokoyama, 1998. Estimation of snowfall, maximum snowdepth and
570 snow cover condition in Japan under global climate change. Seppyo 60 (5),
571 367-378 (in Japanese with English abstract).

572 Ishizaki, N. N., I. Takayabu, M. Oh'izumi, H. Sasaki, K. Dairaku, S. Iizuka, F. Kimura,
573 H. Kusaka, S. A. Adachi, K. Kurihara, K. Murazaki, and K. Tanaka, 2012.
574 Improved performance of simulated Japanese climate with a multi-model
575 ensemble. J. Meteor. Soc. Japan 90(2), 325‐254, doi: 10.2151/jmsj.2012-206.
576 Jordan, R., 1991. A one-dimensional temperature model for a snow cover. Technical
577 Documentation for SNTHERM.89. Special Report 657, U.S. Army Cold
578 Regions Research and Engineering Laboratory, Hanover, NH., 64 pp.
579 Karpechko, A. Y., 2010. Uncertainties in future climate attributable to uncertainties in
580 future Northern Annular Mode trend, Geophys. Res. Let. 37, doi:
581 10.1029/2010gl044717.
582 Kimura, F., and A. Kitoh, 2007. Downscaling by pseudo global warming method Report,
583 Research Institute for Humanity and Nature (RIHN), Kyoto, Japan, pp. 43‐46.
584 Kuno, R., and M. Inatsu, 2014. Development of sampling downscaling: a case for
585 wintertime precipitation in Hokkaido. Clim. Dyn. 43 (1-2), 375‐387, doi:
586 10.1007/s00382-014-2060-5.
587 Lazar, B. and Williams, M., 2008. Climate change in western ski areas: Potential
588 changes in the timing of wet avalanches and snow quality for the Aspen ski
589 area in the years 2030 and 2100. Cold Reg. Sci. Technol. 51, 219‐228, doi:

10.1016/j.coldregions.2007.03.015.

Lazar, B., J. Smith, and M. Williams, 2006. Estimating the changes in climate and snow quantity at the Aspen ski area for the years 2030 and 2100, paper presented at 74th Annual Western Snow Conference, Western Snow Conference, Las Cruces, New Mexico.

Lehning, M., P. Bartelt, B. Brown, and C. Fierz, 2002a. A physical SNOATACK model for the Swiss avalanche warning. Part III. Meteorological forcing, thin layer formation and evaluation. Cold Reg. Sci. Technol. 35 (3), 169‐184, doi: 10.1016/s0165-232x(02)00072-1.

Lehning, M., P. Bartelt, B. Brown, C. Fierz, and P. Satyawali, 2002b. A physical SNOWTACK model for the Swiss avalanche warning. Part II. Snow microstructure. Cold Reg. Sci. Technol. 35 (3), 147 ‐ 167, doi: 10.1016/s0165-232x(02)00073-3.

López-Moreno, J. I., S. Goyette, M. Beniston, and B. Alvera, 2008. Sensitivity of the snow energy balance to climatic changes: prediction of snowpack in the Pyrenees in the 21st century. Clim. Res. 36 (3), 203 ‐ 217, doi: 10.3354/cr00747.

López-Moreno, J. I., J. W Pomeroy, J. Revuelto, and S. M. Vicente-Serrano, 2013.

608 Response of snow processes to climate change: spatial variability in a small
609 basin in the Spanish Pyrenees. Hydrol. Process. 27, 2637–2650, doi:
610 10.1002/hyp.9408.
611 Mellander, P.-E., M. O. Löfvenius, and H. Laudon, 2007. Climate change impact on
612 snow and soil temperature in boreal Scots pine stands. Climatic Change 85,
613 179–193, doi: 10.1007/s10584-007-9254-3.
614 Mitter, C., H. Hirashima, and J. Schweizer, 2011. Wet-snow instabilities: comparison of
615 measured and modelled liquid water content and snow stratigraphy. Ann.
616 Glaciol. 52 (58), 201–208, doi: 10.3189/172756411797252077.
617 Monin, A.S., A.M. Obukhov, 1954. Osnovnye zakonomernosti turbulentnogo
618 peremeshivanija v prizemnom sloe atmosfery (Basic laws of turbulent mixing
619 in the atmosphere near the ground). Trudy geofiz. inst. AN SSSR 24(151),
620 163–187.
621 Nakai, S., T. Sato, A. Sato, H. Hirashima, M. Nemoto, H. Motoyoshi, K. Iwamoto, R.
622 Misumi, I. Kamiishi, T. Kobayashi, K. Kosugi, S. Yamaguchi, O. Abe, and M.
623 Ishizaka, 2012. A Snow Disaster Forecasting System (SDFS) constructed
624 from field observations and laboratory experiments. Cold Reg. Sci. Technol.
625 70, 53–61, doi: 10.1016/j.coldregions.2011.09.002.

626 Nakamura, K., T. Sato, Y. Yamanaka, and K. Nishimura, 2011. Development of method
627 for estimation of changes in snow structure with climate change in Hokkaido,
628 in Cold Region Technology Conference 2011, Sapporo, Hokkaido, Japan, pp.
629 80-85 (in Japanese).
630 Nishimura, K., E. Baba, H. Hirashima, M. Lehning, 2005. Application of the snow
631 cover model SNOWPACK to snow avalanche warning in Niseko, Japan. Cold
632 Reg. Sci. Technol. 43, 62-70, doi: 10.1016/j.coldregions.2005.05.007.
633 Niwano, M., T. Aoki, K. Kuchiki, M. Hosaka, and Y. Kodama, 2012. Snow
634 Metamorphism and Albedo Process (SMAP) model for climate studies. Model
635 validation using meteorological and snow impurity data measured at Sapporo,
636 Japan. J. Geophys. Res. 117, F03008, doi: 10.1029/2011JF002239.
637 Ogata, T., H. Ueda, T. Inoue, M. Hayasaki, A. Yoshida, S. Watanabe, M. Kira, M.
638 Ooshiro, and A. Kumai, 2014. Projected future changes in the Asian monsoon.
639 A comparison of CMIP3 and CMIP5 model results. J. Meteorol. Soc. Japan
640 92 (3), 207-225, doi: 10.2151/jmsj.2014-302.
641 Peel, M. C., B. L. Finlayson, and T. A. McMahon, 2007. Updated world map of the
642 Köppen-Geiger climate classification. Hydrol. Earth Sys. Sci. 11 (5), 1633-
643 1644, doi: 10.5194/hess-11-1633-2007.

644 Prudhomme, C., N. Reynard, and S. Crooks, 2002. Downscaling of global climate
645 models for flood frequency analysis: where are we now? Hydrol. Process. 16
646 (6), 1137‐1150, doi: 10.1002/hyp.1054.
647 Rasmus, S., J. Raisanen, and M. Lehning, 2004. Estimating snow conditions in Finland
648 in the late 21st century using the SNOWPACK model with regional climate
649 scenario data as input. Ann. Glaciol. 38, 238 ‐ 244, doi:
650 10.3189/172756404781814843.
651 Roeckner, E., G. Bäuml, L. Bonaventura, R. Brokopf, M. Esch, M. Giorgetta, S.
652 Hagemann, I. Kirchner, L. Kornblueh, E. Manzini, A. Rhodin, U. Schlese, U.
653 Schulzweida, and A. Tompkins, 2003. The atmospheric general circulation
654 model ECHAM5. Part 1. model description Report, MPI for Meteorol,
655 Hamburg, Germany.
656 Rousselot, M., Y. Durand, G. Giraud, L. Merindol, I. Dombrowski-Etchevers, M. Deque,
657 and H. Castebrunet, 2012. Statistical adaptation of ALADIN RCM outputs
658 over the French Alps - application to future climate and snow cover. The
659 Cryosphere 6 (4), 785‐805, doi: 10.5194/tc-6-785-2012.
660 Saito, K., T. Fujita, Y. Yamada, J. Ishida, Y. Kumagai, K. Aranami, S. Ohmori, R.
661 Nagasawa, S. Kumagai, C. Kuroi, T. Katoh, H. Eito, and Y. Yamazaki, 2006.

The operational JMA nonhydrostatic mesoscale model. Mon. Weather Rev. 134(4), 1266‐1298, doi: 10.1175/mwr3120.1.

Shin, Y., K. Takahashi, N. Hanasaki, and Y. Hijioka, 2012. Climate projections of around Japan - Comparison between CMIP3 and CMIP5 model. J. Japan Soc. Civ. Eng., Ser. G (Environmental Research) 68 (5), I_159‐I_169, doi: 10.2208/jscejer.68.I_159. (in Japanese)

Solomon, S., D. Qin, M. Manning, Z. Chen, M. Marquis, K.B. Averyt, M. Tignor, and H.L. Miller (eds.), 2007. Climate change 2007. The physical science basis. Contribution of Working Group I to the Fourth Assessment Report of the Intergovernmental Panel on Climate Change. Cambridge University Press, Cambridge, United Kingdom and New York, NY, USA, 996 pp.

Stocker, T.F., D. Qin, G.-K. Plattner, M. Tignor, S.K. Allen, J. Boschung, A. Nauels, Y. Xia, V. Bex, and P.M. Midgley (eds.), 2014. Climate change 2013. The physical science basis. Contribution of Working Group I to the Fifth assessment report of the Intergovernmental Panel on Climate Change. Cambridge University Press, Cambridge, United Kingdom and New York, NY, USA,1535 pp.

Takano, Y., Y. Tachibana, and K. Iwamoto, 2008. Influences of large-scale atmospheric

680 circulation and local sea surface temperature on convective activity over the
681 Sea of Japan in December. SOLA 4, 113‑116, doi: 10.2151/sola.2008-029.
682 Techel, F. and Pielmeier, C., 2010. Snowpack properties of unstable wet snow slopes:
683 Observations from the Swiss Alps, in International Snow Science Workshop,
684 Lake Tahoe, California, USA, 17‑22 October 2010, 187‑193.
685 Uhlmann, B., S. Goyette, and M. Beniston, 2009. Sensitivity analysis of snow patterns
686 in Swiss ski resorts to shifts in temperature, precipitation and humidity under
687 conditions of climate change. Int. J. Climatol. 29, 1048‑1055, doi:
688 10.1002/joc.1786.
689 Wang, Y. Q., L. R. Leung, J. L. McGregor, D. K. Lee, W. C. Wang, Y. H. Ding, and F.
690 Kimura, 2004. Regional climate modeling: Progress, challenges, and
691 prospects. J. Meteorol. Soc. Japan 82 (6), 1599‑1628, doi:
692 10.2151/jmsj.82.1599.
693 Wilby, R. L., S. P. Charles, E. Zorita, B. Timbal, P. Whetton, and L. O. Mearns, 2004.
694 Guidelines for use of climate scenarios developed from statistical
695 downscaling methods Report, the Intergovernmental Panel on Climate
696 Change (IPCC), Switzerland, 27 pp.
697 Yamaguchi, S., A. Sato, and M. Lehning, 2004. Application of the numerical snowpack

model (SNOWPACK) to the wet-snow region in Japan. Ann. Glaciol. 38 (1), 266–272, doi: 10.3189/172756404781815239.

Figures

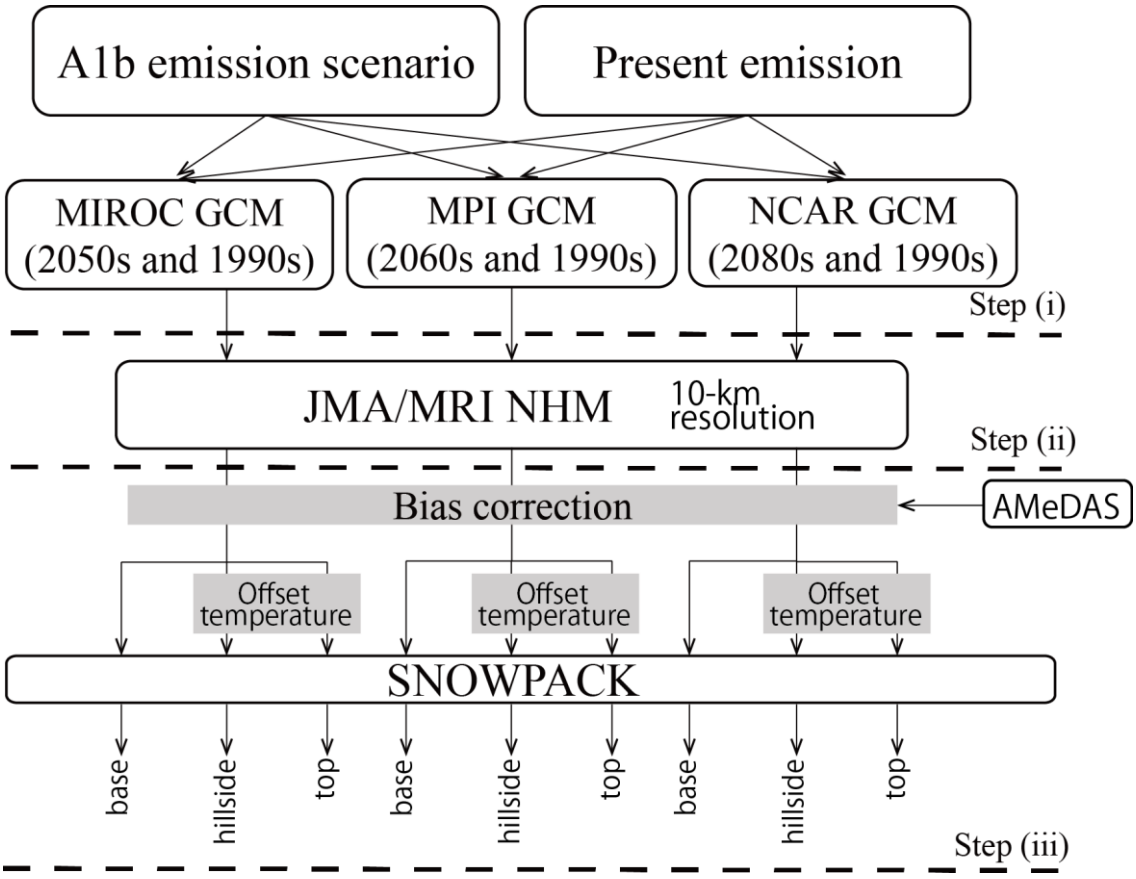
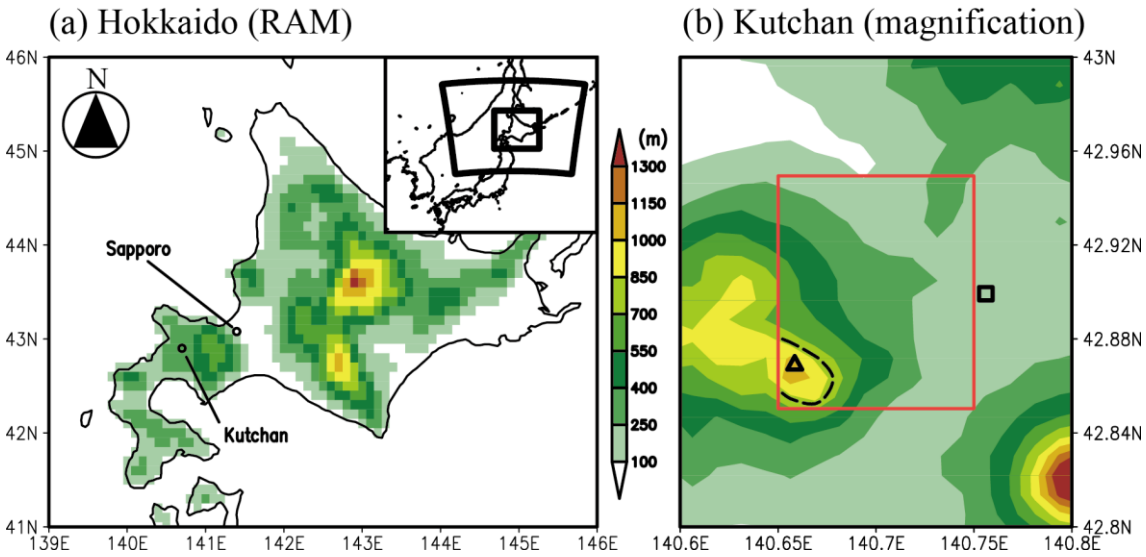


Fig. 1 Flow chart of procedure to assess the future change of snowpack used in this study.



706

707 Fig. 2 (a) Surface height above the sea level given to the regional atmospheric model

708 (RAM) and the location of Hokkaido in the upper right and (b) realistic topography with

709 about 1-km resolution. Outer and inner black solid line in a window of (a) shows RAM's

710 domain calculated and a domain of (a), respectively. The locations of top of Mt. Annupuri

711 (the top; 1,300 m a.s.l.) and AMeDAS station (the base; 173 m a.s.l.) are respectively

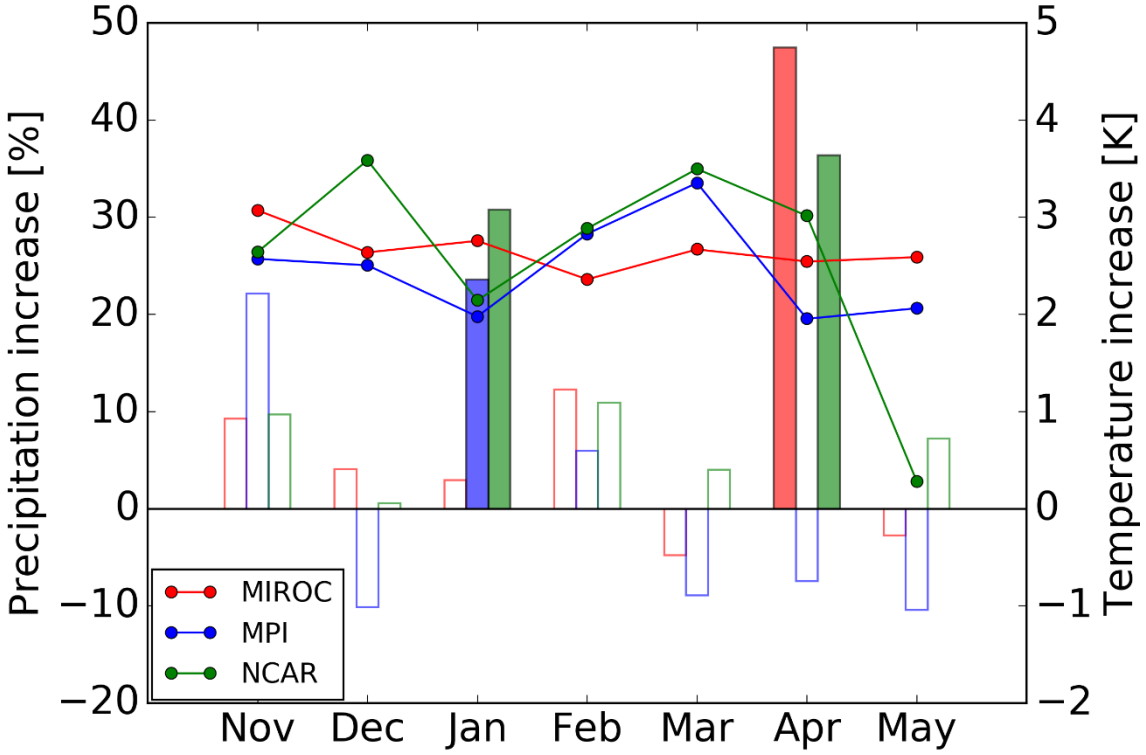
712 indicated with an open triangle and square in (b). Black dashed line in (b) shows an 800

713 m level of height corresponding to the hillside of the mountain slope. Red rectangle in (b)

714 shows the RAM's grid cell of which meteorological data are imposed to the SNOWPACK

715 model. The color-scale is shown between the panels.

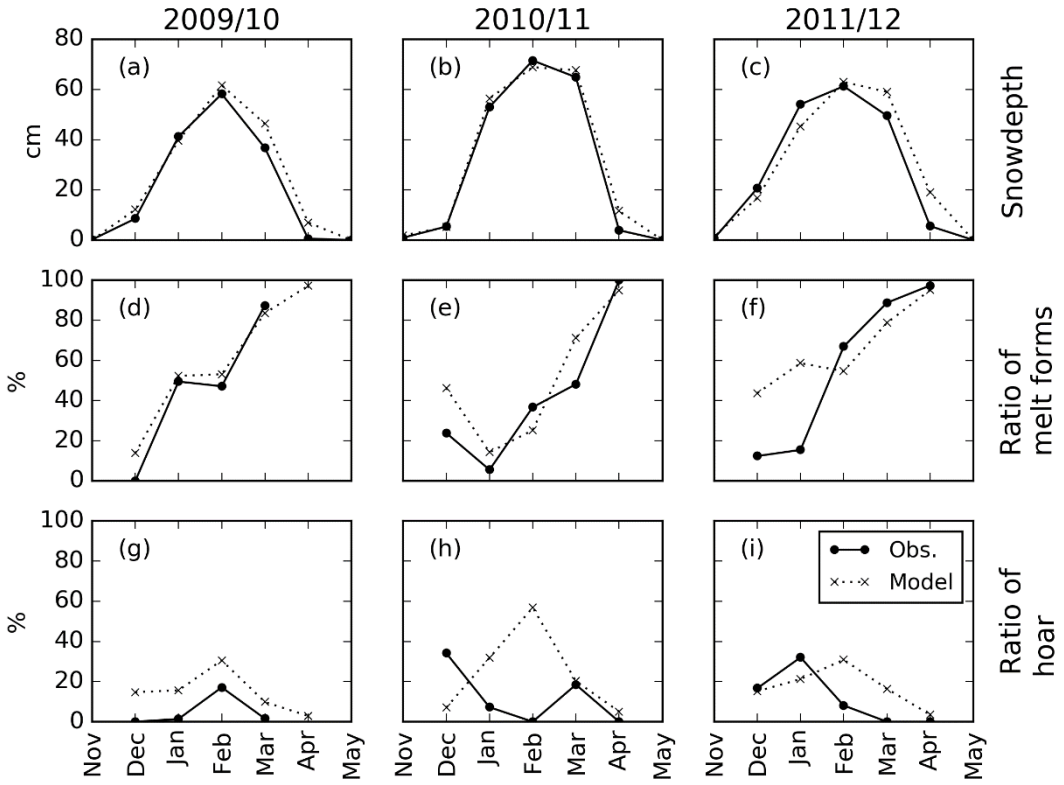
716



717

718 Fig. 3 Global warming response at Kutchan for November to May, based on the
719 dynamical downscaling (DDS) results from (red) the high-resolution version of the
720 Model for Interdisciplinary Research on Climate 3.2 (MIROC), (blue) the
721 fifth-generation atmospheric general-circulation model (GCM) of the
722 Max-Planck-Institut für Meteorologie (ECHAM5/MPI), and (green) version 3 of the
723 Community Climate System Model of the National Center for Atmospheric Research
724 (CCSM3/NCAR). The bar graph shows the increasing rate of monthly precipitation [%;
725 scale on the left] with filled bins denoting a precipitation increase statistically significant
726 at the 10% level. The line graph shows the increase in monthly-mean temperature [K;

scale on the right].



729

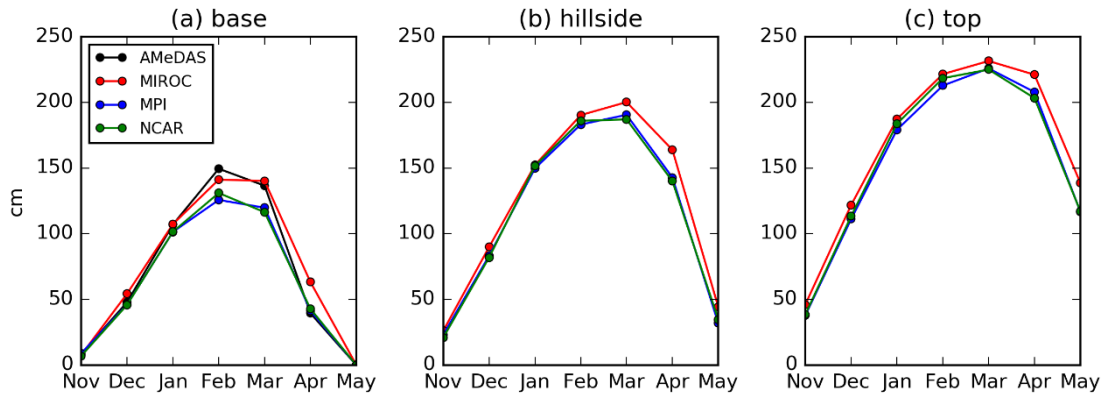
730 Fig. 4 Monthly-mean (a–c) snow depth and the ratios of (d–f) melt forms and (g–i) hoar

731 for all snowpack layers at Sapporo, averaged over the winters of (a, d, g) 2009/10, (b, e, h)

732 2010/11, and (c, f, i) 2011/12. Solid lines with circles show (a-c) AMeDAS and (d–i)

733 snow pit observations; dotted lines with crosses show the SNOWPACK model results.

734



735

736 Fig. 5 Snowpack simulation results with DDS data under the present climate for (red)

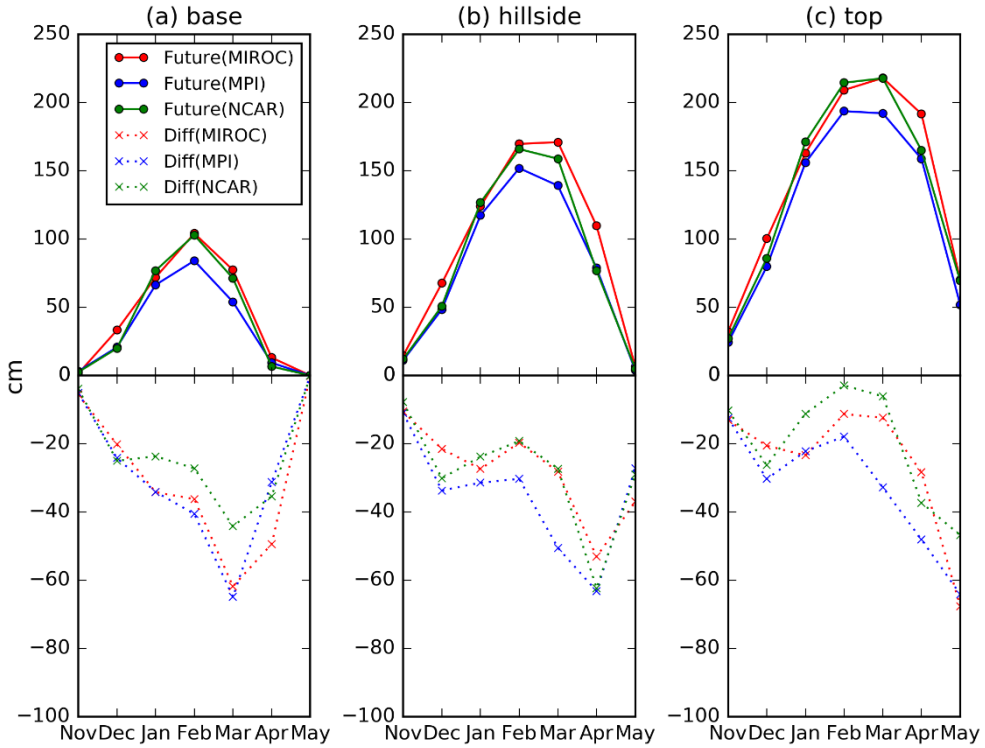
737 MIROC, (green) MPI and (blue) NCAR GCMs. Panels show monthly-mean snow depth

738 on Mt. Annupuri at (a) the base point at 173 m above sea level, (b) the hillside point at 800

739 m, and (c) the top point at 1,300 m. Snow depth observed at the JMA's site at Kutchan is

740 superimposed on (a) in black.

741



742

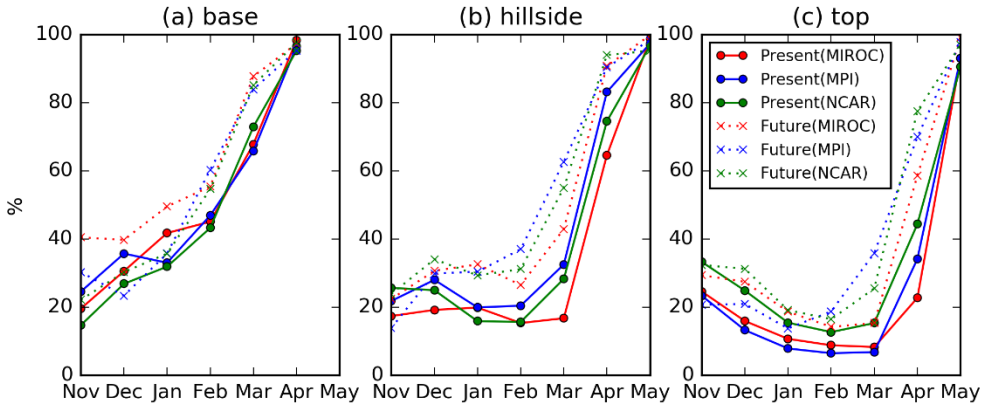
743 Fig. 6 Monthly-mean snow depth in future climate (solid lines) and the difference

744 between present and future climates (dotted lines) at (a) base, (b) hillside, and (c) top

745 points on Mt. Annupuri, based on the DDS data for (red) MIROC, (green) MPI and (blue)

746 NCAR GCMs.

747

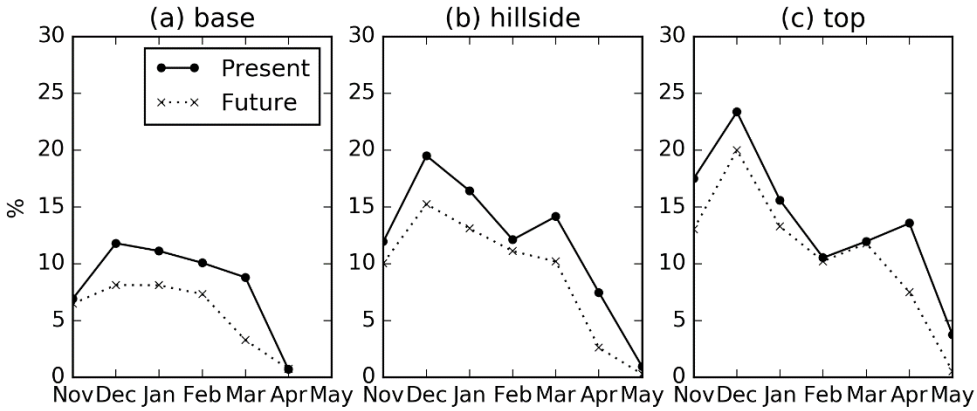


748

749 Fig. 7 The ratio of melt forms at (a) base, (b) hillside, and (c) top points, based on the

750 DDS data under (solid line) present and (dotted) future climates.

751



752

753 Fig. 8 The ratio of hoar at (a) base, (b) hillside, and (c) top, based on the DDS data

754 averaged over all GCM cases under (solid line) present and (dotted) future climates.

755

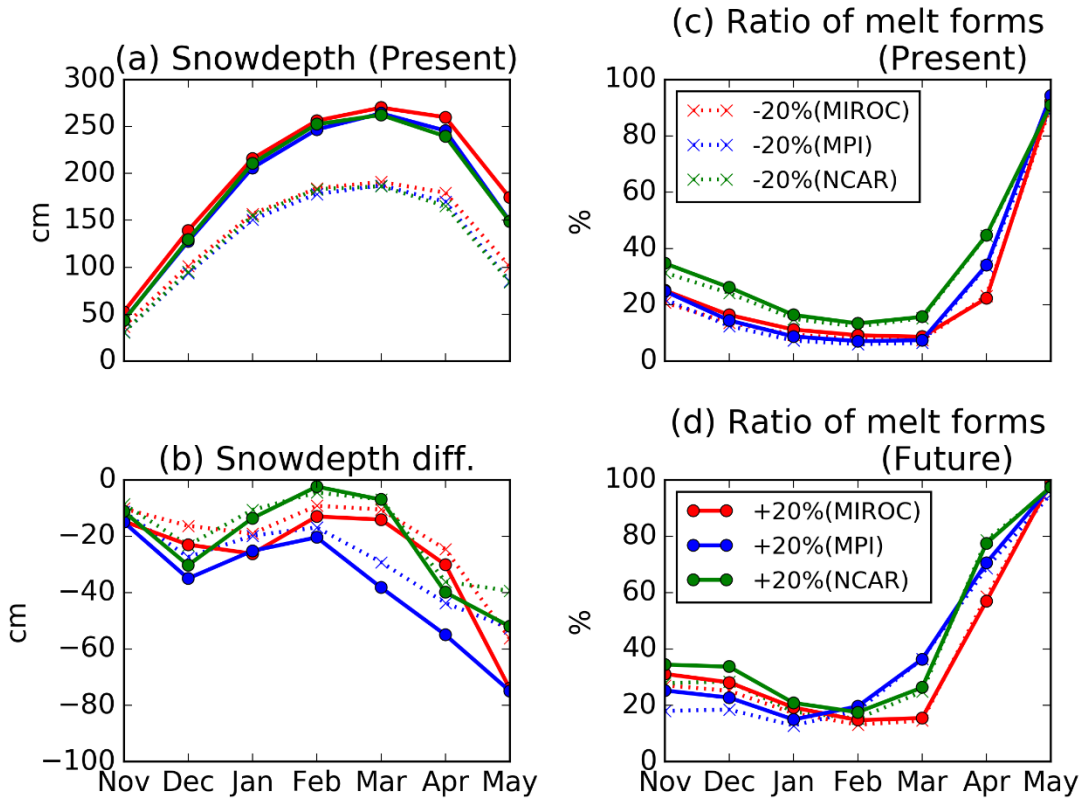
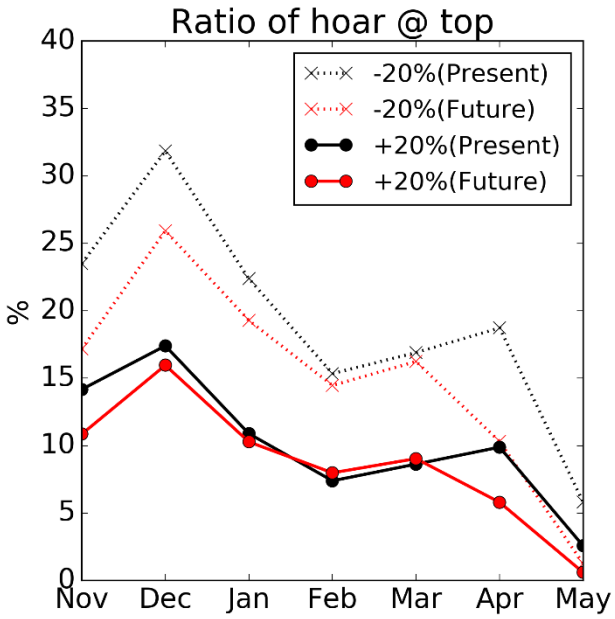


Fig. 9 (a) The monthly-mean snow depth in present climate in (solid line) +20% and (dotted) −20% precipitation experiments. Red, blue, and green lines indicate MIROC's, MPI's, and NCAR's case, respectively. (b) The difference of the snow depth between present and future climate. (c,d) The ratio of melt forms in (c) present and (d) future climate.



763

764 Fig. 10 The ratio of hoar averaged over all GCMs in (black) present and (red) future

765 climate in (solid line) +20% and (dotted line) −20% precipitation experiments.

766